Inter-storm variation in microplastic concentration and polymer type at stormwater outfalls and a bioretention basin

Authors William Boni,[a] Georgia Arbuckle-Keil,[b] N.L. Fahrenfeld[a*]

[a] Civil & Environmental Engineering, Rutgers, The State University of New Jersey, 500 Bartholomew Rd, Piscataway, NJ 08854, USA

[b] Chemistry, Rutgers Camden, 315 Penn St., Camden, NJ 08102, USA

Corresponding author email: nfahrenf@rutgers.edu

Abstract

Microplastics (MP) are a commonly reported pollutant in the freshwater, marine, and soil environment. Few studies to date have reported MP concentrations and polymer types observed in stormwater, particularly not for catchments with separate storm sewers. The objectives of this study were to determine the microplastic concentration, polymer fingerprints, and the inter-storm variation of MP in two stormwater outfalls and a bioretention basin. Composite stormwater samples were collected at each site across three rain events each in catchments with urban and suburban land use. Particles 250 to 2000 μm were collected, separated into two sizes classes, treated with a wet peroxide oxidation, density separated with NaCl, and buoyant particles (fragments, films, and spheres) were collected for analysis with attenuated total reflectance Fourier transform infrared spectroscopy (ATR-FTIR). Significant differences were observed in the total polymer concentrations and profiles between the sampling sites, potentially due to differences in land use within the catchments sampled, but not between size classes. The highest

MP concentrations were observed in samples from the bioretention basin compared to the stormwater outfalls sampled, indicating the potential for green infrastructure to capture MP in the size range studied here. A weak but significant negative correlation was observed between cumulative rainfall (1.5 to 4.5 cm) and MP concentrations but no correlation was observed between antecedent dry days and MP concentrations. These data represent a conservative measure of MP concentrations given that fibers, particles < 250 μm, and non-buoyant particles (i.e., density > 1.2 g/mL) were not targeted, but all targeted particles were analyzed with ATR-FTIR. Overall, these results presented provide insight into the loading and character (size, morphology, polymer type) of buoyant MP particles in stormwater that may be useful in designing mitigation strategies.

Keywords: plastic, runoff, green infrastructure, polymers, FTIR

1.0 Introduction

Increasing reports of plastic pollution of freshwater bodies has drawn attention to understanding the potential pathways of entry in rivers and lakes (Bailey et al., 2021; Fahrenfeld et al., 2019). Generally, plastic particles less than 5mm in size have been operationally defined as microplastics (MP) (Kershaw and Rochman, 2015). MP include primary particles produced in small sizes and secondary MP that result from the degradation of larger plastics via several weathering processes (Guerranti et al., 2019; Li et al., 2018). MP are ubiquitous in the freshwater, marine, and soil environment, and have been found in aquatic organisms such as bivalves, fish, and crustaceans (Shruti et al., 2021). Emissions of MP from municipal wastewater treatment plants have received to date the most attention as a pathway of entry into the aquatic environment, although consensus is growing that conventional wastewater treatment, while not designed to remove these particles, can achieve removal to concentrations below detection in effluent [as recently reviewed by (Conley et al., 2019; Sun et al., 2019)]. Therefore, of particular interest are understudied pathways of entry including stormwater runoff, combined sewer overflows, improperly disposed plastic, land applied biosolids, and other sources that have not yet been characterized (Fahrenfeld et al., 2019; Shruti et al., 2021; SusChem, 2020).

Stormwater is a relatively understudied pathway of entry for MP with concentrations reported for sites in Europe including Paris (Dris et al., 2018) and Sweden (Järlskog et al., 2020), Denmark (Liu et al., 2019), and North American for Tijuana, Mexico (Piñon-Colin et al., 2020), San Francisco, CA (Gilbreath et al., 2019; Werbowski et al., 2021), Toronto (Smyth et al., 2021), and New Jersey, (Bailey et al., 2021), China (Sang et al., 2021), Hong Kong (Mak et al., 2020), and Australia (Ziajahromi et al., 2020). These studies targeted a variety of MP particle size ranges

54 from > 20 μm to 5mm and densities (>1.2–1.8 g/cm), and used a range of analytical approaches,
55 the most common of which were vibrational spectroscopic techniques. Previous work from our
56 research group indicated that stormwater contained MP concentrations of 500–2000μm particles
57 significantly higher than observed in surface waters and comparable to those in wastewater
58 effluent, albeit with a small sample size (Bailey et al. 2021).

59 Of interest for understanding MP in stormwater is not only the concentrations observed in
60 untreated outfalls but also the role of various green and gray infrastructure on reducing MP
61 concentrations. One such green infrastructure (GI) sampled for this study was a bioretention
62 basin. Bioretention basins are a preferred technique to reduce the velocity of stormwater flows
63 (Wang et al., 2021), and they act as a quiescent zone enabling particles to settle and become
64 trapped in the soil medium even if the basin is overflowing. Because wet weather flows
65 contribute to pollutant loading in surface waters (Chen et al., 2020), green infrastructure must be
66 designed to effectively capture particulates without allowing them to be washed out during high
67 flow situations. The few available studies performed to date indicate that GI can be effective at
68 removing particulate matter from stormwater under a variety of flow conditions and are
69 important tools in the protection of waterways (Gilbreath et al., 2019; Smyth et al., 2021;
70 Werbowski et al., 2021).

71 The objectives of this study were to (1) determine the concentration of 250–2000 μm MP in
72 storm- and bioretention basin waters, (2) understand inter-storm variation at our study sites by
73 capturing data for multiple storm events, and (3) characterize the polymer profiles observed. To
74 add to our understanding of MP in stormwater and GI, a field study was performed at two
75 stormwater outfalls and one bioretention basin in a suburban/urban environment. The results

76 presented can provide insight into the relationships between study site, rainfall, and MP
77 concentration and polymer profiles in stormwater and GI.

78 ***2.0 Materials and Methods***

79 ***2.1 Stormwater sampling***

80 Stormwater sampling was performed at two stormwater outfalls in New Brunswick and
81 Piscataway, NJ (named City N and Field P, at end of pipe) and one bioretention basin
82 (Bioretention P, flowing water at outfall) (Fig.1, Fig. S1). The City N outfall collects stormwater
83 from urban landscape with heavily trafficked highways, Field P collects suburban stormwater
84 from recreational fields with artificial turf grass, and Bioretention P is located on a suburban
85 college campus and collects stormwater from an adjacent parking lot and academic buildings.
86 Samples were collected at each outfall for three separate rainfall events. Sampling details are
87 provided in Table 1. Composite stormwater samples were collected in triple washed 1 L glass
88 jars (Ball corp., Broomfield, CO) 20 to 40 min apart during the storm to form a 5 L composite
89 (Fig. S2). Sampling jars were attached to sampling poles lowered by the researchers into the
90 flow stream to collect samples.

91 **Table 1:** Sampling date, precipitation data for the nearest rain gage, and antecedent dry days
92 prior to the storm sampling.

Location	*Date (m/d/yr)*	*Cumulative rainfall (cm)*	*Antecedent dry days*
City N	8/4/20	4.01	3
	10/12/20	3.00	11

Field P	10/29/20	4.50	12
	8/4/20	4.01	3
	10/12/20	3.00	11
	10/29/20	4.50	12
Bioretention P	8/17/20	1.50	4
	8/19/20	1.88	1
	9/29/20	1.85	18

93

94 After collection, samples were transported to the lab in a cooler and stored at 4°C until
95 extraction. Composite samples were wet-sieved using standard soil sieves and the 500–2000 μm
96 and 250–500 μm particles were transferred to glass beakers after being thoroughly rinsed with
97 deionized (DI) water. The beakers were covered with new aluminum foil to prevent
98 contamination. Samples were generally extracted the same day as collection or stored in the dark
99 at 4°C for up to two days prior to extraction. Field blanks were performed with a jar of DI water
100 that was left open during sampling and matrix spikes were performed with known quantities of
101 polyethylene extracted from a personal care product.

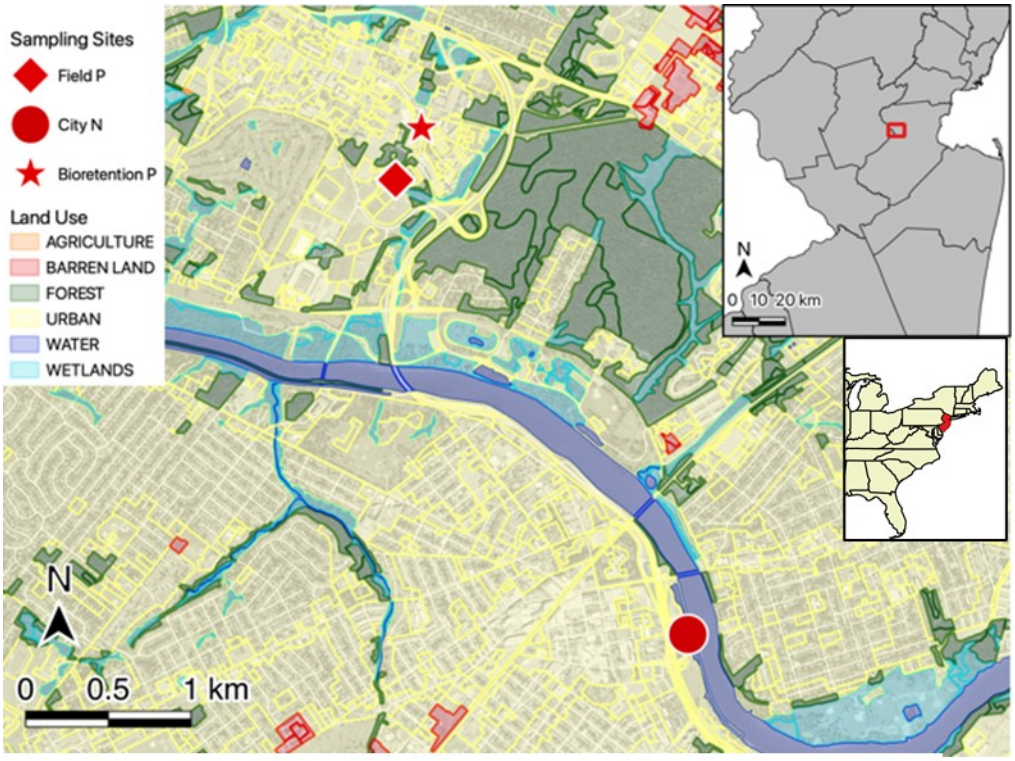

102

103 **Fig. 1** Map of study area showing land-use, water bodies, and locations of sampling sites.
104 Yellow lines on the urban area illustrate roadways. Insert maps show location of the study area
105 in central New Jersey, USA and the location of the state on the US east coast..

106 ***2.2 Oxidation and Density Separation***

107 Organic material was oxidized via a Fenton reaction followed by density separation (Masura et
108 al., 2015). Briefly, the volume of each beaker was brought to 50 mL with distilled water, then 20
109 mL of 0.05 M Fe (II) solution and 20 mL 30% hydrogen peroxide were added to each beaker.
110 After 5 min of reacting at ambient temperature, the samples were heated to 65°C on a hot plate
111 while being stirred at approximately 120 rpm covered with watch glasses to prevent
112 contamination. Beakers were held at 65°C for 30 min followed by addition of salt (6 g NaCl was

added to each beaker per 20 mL of solution, to create a solution of density 1.2 g/mL) to facilitate density separation. The choice of NaCl here was consistent with the NOAA method applied and facilitated comparison with previous work from our lab (Bailey et al., 2021) and the loss of denser particles with this method is discussed below. After the addition of salt, samples were stirred for another 30 min at 65°C to ensure the NaCl was dissolved fully and that the bubbling had stopped. Samples were transferred to glass funnels topped with aluminum foil to prevent contamination. Surgical tubing was attached to the funnel bottom and closed with a clamp. After allowing the solution to settle for 24 hours, the settled solids were carefully drained from the bottom of the funnel, and the supernatant was filtered through new 63 μm stainless steel mesh (TWP, Berkeley, CA). Particles retained on the mesh were rinsed with DI water, and the mesh was placed in glass petri dishes with glass covers to dry.

2.3 Chemical analysis

Particles were analyzed using Attenuated Total Reflectance Fourier Transform Infrared Spectroscopy (ATR-FTIR) Bruker Alpha spectrometer (Bruker Optics, Billerica, MA) with a single bounce diamond internal reflection element (IRE) ATR accessory and a DTGS (Deuterated Triglycine Sulfate) detector. Physical descriptions (i.e., color and morphology) of the particles were recorded, and selected particles were photographed with a cellphone camera (Fig. S3). All particles in a sample were transferred to the IRE using a metal scalpel and metal tweezers (therefore, particles < 250 μm were not analyzed using this method as they could not be reliably transferred to the IRE without losses). Spectra were collected with 32 scans performed per particle at a resolution of 4cm^{-1} in the wavenumber range of 4000 to 400 cm^{-1}. Background scans were performed periodically to reduce noise. FTIR spectra were analyzed using

Systematic Identification of MicroPLastics in the Environment (siMPle) version 1.1.β which contains a database of polymer spectra (Version 1.02, (Primpke et al., 2018)). The software compares the spectrum of an unknown particle to a reference database of 326 polymer spectra. The result is a correlation value between zero and one, with one being a 100% match to the library spectra, and zero representing no correlation. The top five polymer matches were recorded for each particle, and peaks were checked manually against reference spectra to confirm polymer type. In general, particles that scored above a 50% match for a given polymer were matched to that polymer type and categorized.

2.4 Data Analysis

Statistical analysis was performed using the R (www.r-project.org) vegan package (https://cran.r-project.org/web/packages/vegan/) as well as the pairwise.Adonis function (github.com/pmartinezarbizu/pairwiseAdonis). A Shapiro-Wilk test confirmed that the microplastic concentration data were not normal. A paired Wilcoxon rank sum test was performed to compare concentrations for the two size classes. To test for differences in total microplastic concentrations between sites, a Kruskal-Wallis test was performed with a post hoc pairwise t-test with a Bonferroni correction for multiple comparisons. Correlations were tested between microplastic concentration and cumulative rainfall using a Spearman test, and a linear regression was performed in R. To understand the relative importance of sampling site and climate factors (rainfall, antecedent dry days), randomForest was performed on the total MP concentration. A Pairwise PERMANOVA test was performed in order to evaluate each variable's contribution to polymer profiles observed. Like the post hoc pairwise t- test, the

pairwise.Adonis function adjusts p values for multiple comparisons using a Bonferroni correction after performing the PERMANOVA.

In order to visually represent the polymer fingerprints and analyze polymer profiles from the pairwise PERMANOVA test, non-metric multidimensional scaling (nMDS) was performed on the data. This was done in R using the metaMDS function with two reduced dimensions. The nMDS processing provided a visual method to interpret the polymer profiles observed. In addition, a stress value was computed by the metaMDS function to determine the trustworthiness of the visualization and the fit achieved in the regression procedure.

3.0 Results

3.1 Microplastic concentrations

Microplastics were observed in both size classes (250–500 μm and 500–2000 μm) for each of the six stormwater and three bioretention basin samples collected during rainfall events totaling 1.5–4.5 cm of cumulative rainfall (Table 1). Average (± standard deviation) total 250–2000 μm MP concentration observed across storms were 0.80±0.33 MP/L (BBR), 0.30±0.10 MP/L (City N), and 0.37±0.23 MP/L (Field P) with the highest total concentrations observed in the bioretention basin compared to other sites (both $p<0.022$, posthoc pairwise t-test) (Fig. 2). Differences were not observed in the concentrations of the two particle size classes studied across sites ($p=0.43$, paired Wilcoxon). MP morphologies included fragments, films, and foams, with the most commonly observed morphology being fragments. No MP were observed in the field blanks, and the average recovery of matrix spikes was 97% ± 6%.

176 To understand the factors associated with microplastic concentration, correlations were tested
177 and a relationship was observed between microplastic concentration and cumulative rainfall
178 (Spearman correlation, ρ= -0.53, p=0.014). The results of the linear regression (Fig. S4) show a
179 weak negative relationship between cumulative rainfall and MP concentration (p=0.014, adj.
180 R^2=0.23). Random forest analysis indicated that 58.8% of the variance in MP concentration
181 could be explained by sampling site, cumulative rainfall, and antecedent dry days representing
182 9.57, 9.07, and 2.22 percent increase in mean square error, respectively.

183

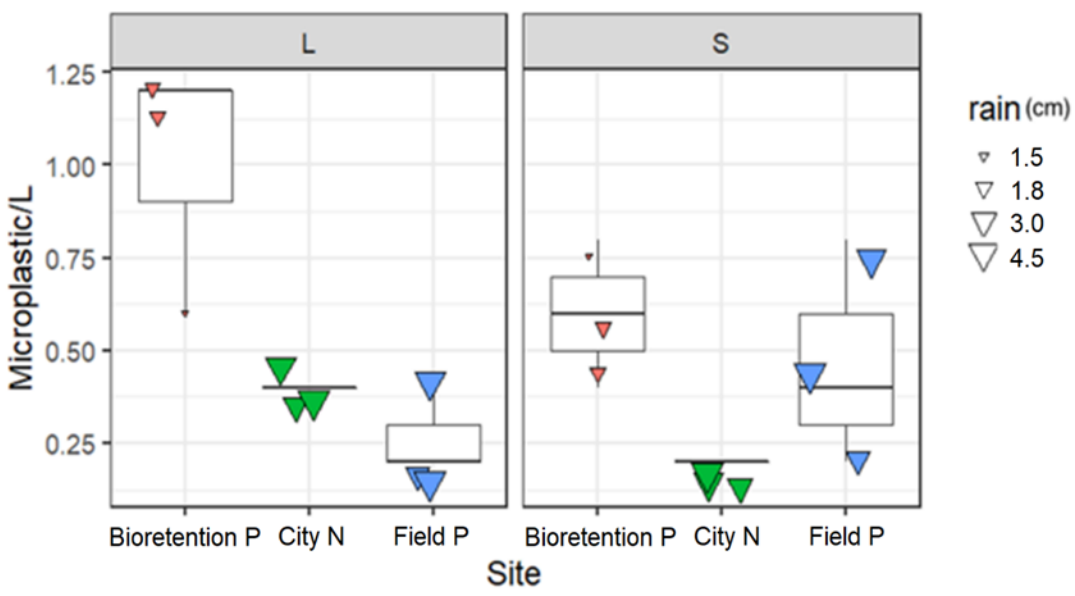

184

185 **Fig. 2** Boxplots of MP concentrations (MP particles per liter of water) observed in the
186 bioretention basin and stormwater for City N and Field P for 500–2000 µm ("L") and 250–500
187 µm ("S") particles. Size of the triangles for the jitter plot corresponds to the cumulative rainfall
188 observed during the storm event (N=3 per site).

3.1 Polymers observed

Several different polymer types were observed, both manmade and natural in origin. Manmade polymers were divided into 7 categories, including polyethylene (PE), polystyrene (PS), polypropylene (PP), copolymer of ethylene-ethyl acrylate (COPOLY), polyethylene terephthalate (PETE), and acrylonitrile styrene-butadiene (ABS, Fig. 3) based on top match in siMPle database. The copolymer ethylene ethyl acrylate was the most commonly observed polymer (N=25 COPOLY /44 MP total), followed by polyethylene (N=6) across sites. Of the 196 particles analyzed, 44 particles (22%) were identified as MP. Example spectra are shown in Fig. S5. Common non-anthropogenic polymers detected had high similarity to cellulose and beeswax. These particles are resistant to the oxidation procedure and sometimes visually resembled plastic, especially in the form of small fragments, underscoring the need for spectroscopic analysis. The fingerprint region of the spectra varied somewhat for the 25 COPOLY MP spectra and identification as copolymer of ethylene-ethyl acrylate was made based on the top match of ~0.75 vs. 0.94 for PE. The lower hit match may indicate surface oxidation or mixed copolymer composition.

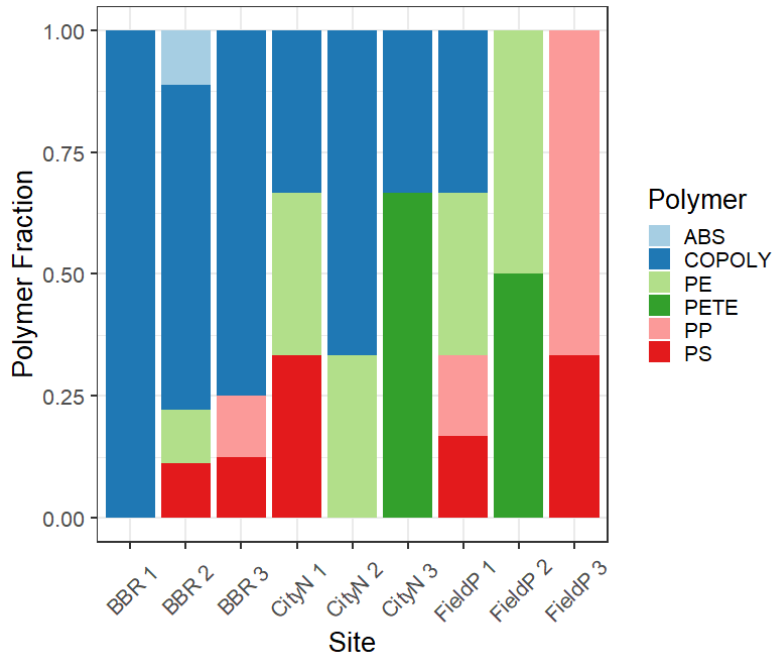

204

205 **Fig. 3** Fraction of the total MP observed represented by each polymer type, by sampling site and
206 storm (numbered 1–3). BBR is the Bioretention P. Polymer types are abbreviated ABS for
207 acrylonitrile styrene-butadiene, COPOLY for copolymer of ethylene-ethyl acrylate, PE for
208 polyethylene, PETE for polyethylene terephthalate, PP for Polypropylene, and PS for
209 polystyrene. Replicates represent different storm events (N=3).

210 The polymer profiles observed varied between the bioretention basin compared to the two other
211 sites (Field P vs Bioretention P p=0.03, City N vs Bioretention P p=0.009, pairwise
212 PERMANOVA). City N and Field P did not have significant difference in composition (p=0.76).
213 Polymer profiles did not vary by storm event at a given site (all adj p > 0.86) or between the
214 small and large size class (p=0.88, PERMANOVA). nMDS was used to visualize the differences
215 in polymer profiles, achieving a stress of 0.109, suggesting this is an acceptable representation of
216 the data in two dimensions. The nMDS plot shows that Bioretention P had a different polymer

profile compared to Field P or City N (Fig. 4), whereas no such clustering was observed as a function of size class and storm event for a given site.

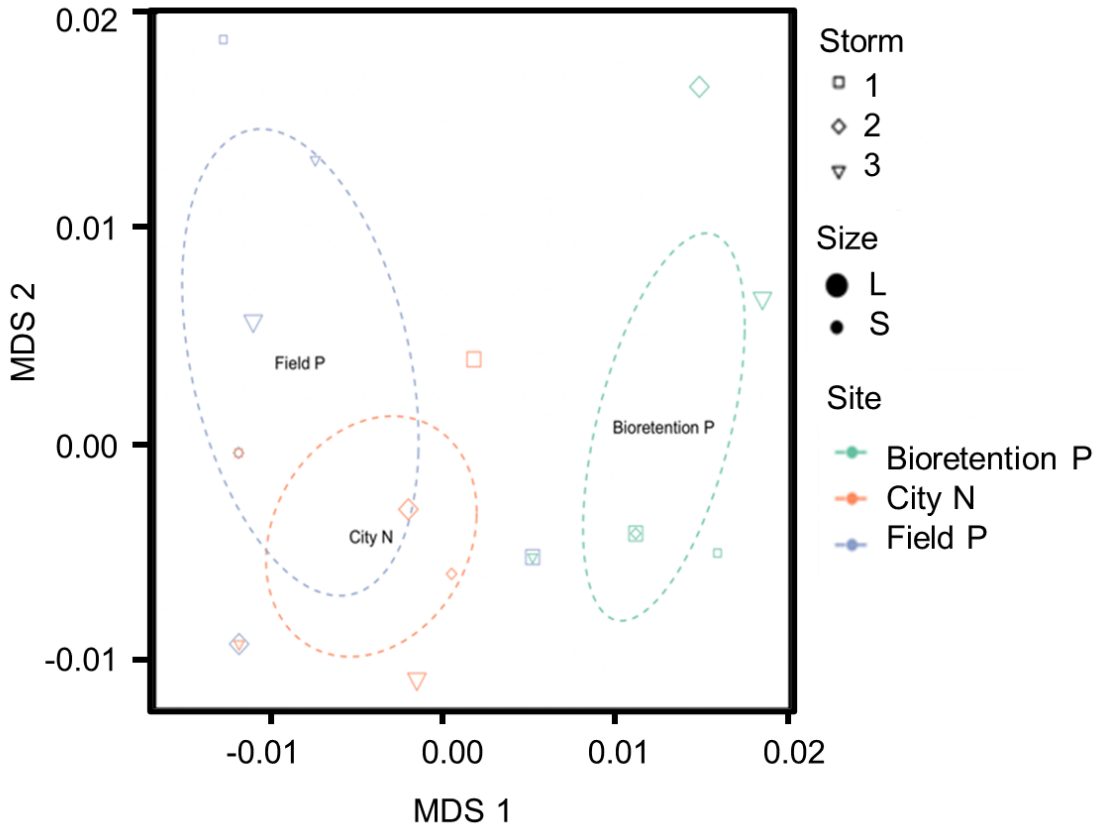

Fig. 4 nMDS visualization showing the Bioretention P with a distinct polymer profile compared to City N and Field P. Size of data points corresponds to the 500–2000 µm ("L") and 250–500 µm ("S") particle size class. Shape corresponds to the storm. Ellipses represent a 95% confidence interval around the centroids for data from a given site.

4.0 Discussion

4.1 Stormwater as a source of MP

MP were observed in all stormwater samples in both size classes studied (0.30–0.90 MP/L, 250–500 and 500–2000 μm) with significantly more MP observed in the bioretention basin compared to the two storm outfalls. The high concentrations observed in the bioretention basin can likely be explained by proximity to potential sources and pooling of stormwater. The bioretention basin is located next to a parking lot and receives runoff directly from it. Roads, parking lots, and other impervious surfaces are known to increase stormwater volume and pollutant loading to the environment (Zhou et al., 2021). Because urban stormwater is a known source of MP, land cover and impervious surface area in a given catchment are important factors influencing the MP concentration reaching surface waters. Field P and City N both receive runoff from impervious surfaces, but also feature much more permeable cover in the immediate vicinity, with City N being located in a park, and Field P receiving runoff from sports fields along with a two-lane road. The higher concentrations observed at the bioretention basin were also likely influenced by the storm events captured at this site, which happened to have lower cumulative rainfall.

MP concentrations observed in this study are reasonably consistent with recent publications investigating MP in untreated urban runoff: 2 to 16 MP/L in Paris for 100–5000 μm (Dris et al., 2018), 0.4 to 3.2 MP/L in San Francisco for > 125 μm (Gilbreath et al., 2019), 1.1 to 24.6 MP/L for > 125 μm (Werbowski 2021), 1–10 MP/L in Sweden for > 20 μm (Järlskog et al., 2020), and 0.4 to 0.6 MP/L for 500–2000 μm in New York / New Jersey (Bailey et al., 2021). MP concentrations reported in stormwater are highly variable, ranging about three orders of magnitude (Koutnik et al., 2021; Shruti et al., 2021). The MP concentrations from this study are on the lower end of reported values in the literature, which may be explained by (1) our smaller size range and (2) exclusion of fiber morphology during analysis, (3) the use of NaCl (1.2 g/mL)

as a density separation medium instead of a more dense solution such as $CaCl_2$ or NaI, (4) the use of spectroscopic analysis for confirmation of polymer type (assuming the potential for overestimation in studies relying upon visual ID) (Lenz et al., 2015), and (5) the presence of a separate storm and sanitary sewer system in the study area. First, the range of size classes targeted for analysis can impact the reported MP concentrations with some studies reporting analysis of particles as small as 0.01 μm, and therefore having a higher number of MP measured per liter (Koutnik et al., 2021; Shruti et al., 2021). Next (2), previous studies in San Francisco, Tijuana, and Paris were all in catchments with combined sewer systems, and this is reflected in the high fiber concentrations of their samples. The study performed in Tijuana analyzed particles including fibers > 25μm in size and found 88–275 particles/L (Piñon-Colin et al., 2020). However, over 80% of the MP found were fibers, which were not analyzed in this study. The authors noted that the high level of fibers is likely due to combined sewer overflows during storm events, as wastewater is known to contain high levels of MP fiber contamination (Conley et al., 2019; Fahrenfeld et al., 2019; Zhang et al., 2021).

Differences in experimental and analytical methods may also explain why this study found MP concentrations lower than others in the literature. The salt used for density separation (3) can alter the polymer profile observed in the buoyant particles. For example, using sodium iodide (density, ρ=1.8g/mL) rather than sodium chloride (ρ=1.2g/mL) can help capture higher density polymers such as PVC that the methods used in this study are unable to recover (Shruti et al., 2021). Likewise, Gilbreath *et al*. and Werbowski *et al.* used a solution of $CaCl_2$ (1.4 g/mL) for density separation, allowing for recovery of higher density polymers that could contribute to the higher MP concentrations observed. Finally (4), some studies relied upon visual identification

(e.g., the study from Sweden) and visual identification has been reported to be prone to false positives (Lenz et al., 2015; Song et al., 2015; Ziajahromi et al., 2017) and false negatives (Song et al., 2015) particularly for particles in small size classes and with clear color. Other studies which included chemical identification have performed analysis only on a subset of particles for polymer identification, often due to high particle concentrations or large sample volumes on the order of hundreds of liters, whereas in the present study we were able to analyze all particles in the storm samples, albeit with a smaller sample volume.

Comparisons between the range of concentrations of MP in pathways of entry to surface waters can help inform mass balances to surface waters. Comparing the 500–2000μm observations to results from our recent survey of the Hudson Raritan Estuary, the stormwater samples collected in the present study had lower concentrations of MP compared to wastewater influent (0.333–2.25 MP/L, relevant during combined and sanitary sewer overflows), and comparable concentrations to wastewater effluent (<0.001–0.25 MP/L) (Fahrenfeld et al., 2019; Zhang et al., 2021) and surface water concentrations (<0.001 to 0.003 microplastics/L) (Bailey et al., 2021). Concentration differences between studies can be explained by the factors detailed above (e.g., differences in size class or morphology analyzed, density separation medium, etc.) in addition to local factors such as land use, climate, and whether or not the samples were from a combined sewer or separate storm sewer. Sampling was also performed during one season during the COVID-19 pandemic when foot and road traffic were lower than normal, also potentially impacting the results reported here.

4.2 Prevalent polymer types in stormwater

Polymer types observed in the NJ stormwater were consistent with other investigations of urban runoff. Polyethylene is the most commonly reported polymer across all environmental matrices, especially in studies that used saturated NaCl for density separation (Bailey et al., 2021; Piñon-Colin et al., 2020). An analysis of 14 studies that sampled stormwater found acrylates and polyethylene to be most common polymer types in urban canals and stormwater (Koutnik et al., 2021). As mentioned above, researchers that used a solution of higher density such as $ZnCl_2$ (1.6–1.8 g/mL) or NaI (> 1.8 g/mL) were able to recover denser polymers such as PVC in addition to PE and PP. Likewise, using higher density solutions may also capture more polymers associated with road tire wear, such as ABS observed by others (Kole et al., 2017).

The nMDS and PERMANOVA analyses show that the bioretention basin contained a unique polymer fingerprint compared to the two stormwater outfalls. Factors such as differences in morphology or differences in land use (described above) contributing to the unique population of polymers in the bioretention basin. For example, a particle of acrylonitrile styrene-butadiene, likely worn from a car tire, was found in the waters of the bioretention basin, likely due to the basin's proximity to vehicle traffic. The highest number of particles identified as polypropylene (N=2) and polyethylene (N=3) were found near Field P, which is largely covered with artificial turf. This is important to note because artificial turf mats are made most commonly from polyethylene and polypropylene (Magnusson and Mácsik, 2017) meaning this type of ground cover may contribute to MP loading.

4.3 Relationship between MP concentrations in stormwater and precipitation

Of interest is not only connections to land use, but also precipitation events. The negative correlation observed between cumulative rainfall and total MP concentration could be explained by the potential for storms with greater runoff volume to dilute the MP concentrations observed. Antecedent dry days were not correlated with MP concentration, which is likely due to the relatively short dry periods observed during the sampling, with the maximum duration of dry weather measuring 18 days. Studies that found a correlation between antecedent dry days and MP concentration had much longer periods of dry weather, on the order of several months (Piñon-Colin et al., 2020; Smyth et al., 2021).

4.4 Implications for MP removal from stormwater

The observations of higher MP concentrations in the bioretention basin appear to be in agreement with recent research showing that green infrastructure can improve stormwater quality by removing microparticles in general (Chen et al., 2020; Liu et al., 2019; Smyth et al., 2021). One would expect properly designed bioretention basins and rain gardens to be effective at removing particulate pollutants (Lucke and Nichols, 2015) such as MP by filtering out microparticles as the water infiltrates into the sediment (Gilbreath et al., 2019; Lucke and Nichols, 2015). Bioretention basins are designed to reduce the velocity of stormwater flows (Wang et al., 2021), and they act as a quiescent zone enabling particles to become trapped in the soil medium even if the basin is overflowing. Because wet weather flows contribute to pollutant loading in surface waters (Chen et al., 2020), green infrastructure must be designed to effectively capture particulates without allowing them to be washed out during high flow situations. Many stormwater treatment techniques are effective at removing total suspended solids (TSS) and heavy metal particulates (Lucke and Nichols, 2015), and a growing body of evidence shows that

this reduction applies to other particulate matter such as MP (Chen et al., 2020; Gilbreath et al., 2019; Smyth et al., 2021). This phenomenon is analogous to WWTP's effectiveness at removing MP despite not being specifically designed for the purpose (Conley et al., 2019; Fahrenfeld et al., 2019; Sun et al., 2019). The ultimate fate of MP trapped by bioretention basins would likely depend on specifics of the infrastructure including the maintenance (or lack thereof) with particle removal and landfilling potential for those getting regular cleaning and/or the opportunity for burying, UV degradation, biological uptake by terrestrial organisms, and/or resuspension into runoff/air.

5.0 Conclusion

This study further supports the notion that stormwater runoff is a source of MP in the environment with a negative relationship between runoff volume and MP concentration. Sampling site and cumulative rainfall were both found to explain the variance in the MP concentration data. The polymer profiles varied more between sampling sites than storm-to-storm for a given site, underscoring the role of location / land use. Understanding the concentration and character of MP in stormwater and green infrastructure as presented here are important for determining the most relevant sources of MP and can inform the design and/or predicted performance of GI and stormwater management systems.

6.0 Acknowledgements

Funding for this project came from a School of Engineering Fellowship to William Boni, and NSF Grant # 1917676. The authors wish to thank Karli Sipps for assistance with spectroscopic analysis.

References

Bailey K, Sipps K, Saba GK, Arbuckle-Keil G, Chant RJ, Fahrenfeld NL. Quantification and composition of microplastics in the Raritan Hudson Estuary: comparison to pathways of entry and implications for fate. Chemosphere 2021: 129886.

Chen H, Jia Q, Zhao X, Li L, Nie Y, Liu H, et al. The occurrence of microplastics in water bodies in urban agglomerations: Impacts of drainage system overflow in wet weather, catchment land-uses, and environmental management practices. Water Research 2020; 183: 116073.

Conley K, Clum A, Deepe J, Lane H, Beckingham B. Wastewater treatment plants as a source of microplastics to an urban estuary: Removal efficiencies and loading per capita over one year. Water Research X 2019; 3: 100030.

Dris R, Gasperi J, Tassin B. Sources and fate of microplastics in urban areas: a focus on Paris Megacity. Freshwater Microplastics. Springer, Cham, 2018, pp. 69-83.

Fahrenfeld NL, Arbuckle-Keil G, Naderi Beni N, Bartelt-Hunt SL. Source tracking microplastics in the freshwater environment. TrAC Trends in Analytical Chemistry 2019; 112: 248-254.

Gilbreath A, McKee L, Shimabuku I, Lin D, Werbowski LM, Zhu X, et al. Multiyear Water Quality Performance and Mass Accumulation of PCBs, Mercury, Methylmercury, Copper, and Microplastics in a Bioretention Rain Garden. Journal of Sustainable Water in the Built Environment 2019; 5: 04019004.

Guerranti C, Martellini T, Perra G, Scopetani C, Cincinelli A. Microplastics in cosmetics: Environmental issues and needs for global bans. Environmental Toxicology and Pharmacology 2019; 68: 75-79.

Järlskog I, Strömvall A-M, Magnusson K, Gustafsson M, Polukarova M, Galfi H, et al. Occurrence of tire and bitumen wear microplastics on urban streets and in sweepsand and washwater. Science of The Total Environment 2020; 729: 138950.

Kershaw P, Rochman C. Sources, fate and effects of microplastics in the marine environment: part 2 of a global assessment. Reports and studies-IMO/FAO/Unesco-IOC/WMO/IAEA/UN/UNEP Joint Group of Experts on the Scientific Aspects of Marine Environmental Protection (GESAMP) eng no. 93 2015.

Kole PJ, Löhr AJ, Van Belleghem F, Ragas A. Wear and tear of tyres: A stealthy source of microplastics in the environment. International Journal of Environmental Research and Public Health 2017; 14: 1265.

Koutnik VS, Leonard J, Alkidim S, DePrima FJ, Ravi S, Hoek EMV, et al. Distribution of microplastics in soil and freshwater environments: Global analysis and framework for transport modeling. Environmental Pollution 2021; 274: 116552.

388 Lenz R, Enders K, Stedmon CA, Mackenzie DMA, Nielsen TG. A critical assessment of visual
389 identification of marine microplastic using Raman spectroscopy for analysis improvement.
390 Marine Pollution Bulletin 2015; 100: 82-91.

391 Li J, Liu H, Paul Chen J. Microplastics in freshwater systems: A review on occurrence, environmental
392 effects, and methods for microplastics detection. Water Research 2018; 137: 362-374.

393 Liu F, Vianello A, Vollertsen J. Retention of microplastics in sediments of urban and highway stormwater
394 retention ponds. Environmental Pollution 2019; 255: 113335.

395 Lucke T, Nichols PWB. The pollution removal and stormwater reduction performance of street-side
396 bioretention basins after ten years in operation. Science of The Total Environment 2015; 536:
397 784-792.

398 Magnusson S, Mácsik J. Analysis of energy use and emissions of greenhouse gases, metals and organic
399 substances from construction materials used for artificial turf. Resources, Conservation and
400 Recycling 2017; 122: 362-372.

401 Mak CW, Tsang YY, Leung MM-L, Fang JK-H, Chan KM. Microplastics from effluents of sewage
402 treatment works and stormwater discharging into the Victoria Harbor, Hong Kong. Marine
403 Pollution Bulletin 2020; 157: 111181.

404 Masura J, Baker JE, Foster GD, Arthur C, Herring C. Laboratory methods for the analysis of
405 microplastics in the marine environment: recommendations for quantifying synthetic particles in
406 waters and sediments. NOAA Technical Memorandum NOS-OR&R-48 2015.

407 Piñon-Colin TdJ, Rodriguez-Jimenez R, Rogel-Hernandez E, Alvarez-Andrade A, Wakida FT.
408 Microplastics in stormwater runoff in a semiarid region, Tijuana, Mexico. Science of The Total
409 Environment 2020; 704: 135411.

410 Primpke S, Wirth M, Lorenz C, Gerdts G. Reference database design for the automated analysis of
411 microplastic samples based on Fourier transform infrared (FTIR) spectroscopy. Analytical and
412 Bioanalytical Chemistry 2018; 410: 5131-5141.

413 Rodrigues MO, Gonçalves AMM, Gonçalves FJM, Abrantes N. Improving cost-efficiency for MPs
414 density separation by zinc chloride reuse. MethodsX 2020; 7: 100785.

415 Sang W, Chen Z, Mei L, Hao S, Zhan C, Zhang Wb, et al. The abundance and characteristics of
416 microplastics in rainwater pipelines in Wuhan, China. Science of The Total Environment 2021;
417 755: 142606.

418 Shruti VC, Pérez-Guevara F, ElizaldeMartínez I, Kutralam-Muniasamy G. Current trends and analytical
419 methods for evaluation of microplastics in stormwater. Trends in Environmental Analytical
420 Chemistry 2021: e00123.

421 Smyth K, Drake J, Li Y, Rochman C, Van Seters T, Passeport E. Bioretention cells remove microplastics
422 from urban stormwater. Water Research 2021; 191: 116785.

Song YK, Hong SH, Jang M, Han GM, Rani M, Lee J, et al. A comparison of microscopic and spectroscopic identification methods for analysis of microplastics in environmental samples. Marine Pollution Bulletin 2015; 93: 202-209.

Sun J, Dai X, Wang Q, van Loosdrecht MCM, Ni B-J. Microplastics in wastewater treatment plants: Detection, occurrence and removal. Water Research 2019; 152: 21-37.

SusChem. Sustainable Plastics Strategy. PlasticsEurope Association of Plastics Manufacturers, Brussels, Belgium, 2020.

Wang M, Zhang D, Wang Z, Zhou S, Tan SK. Long-term performance of bioretention systems in storm runoff management under climate change and life-cycle condition. Sustainable Cities and Society 2021; 65: 102598.

Werbowski LM, Gilbreath AN, Munno K, Zhu X, Grbic J, Wu T, et al. Urban Stormwater Runoff: A Major Pathway for Anthropogenic Particles, Black Rubbery Fragments, and Other Types of Microplastics to Urban Receiving Waters. ACS ES&T Water 2021.

Zhang L, Liu J, Xie Y, Zhong S, Gao P. Occurrence and removal of microplastics from wastewater treatment plants in a typical tourist city in China. Journal of Cleaner Production 2021; 291: 125968.

Zhou L, Shen G, Li C, Chen T, Li S, Brown R. Impacts of land covers on stormwater runoff and urban development: A land use and parcel based regression approach. Land Use Policy 2021; 103: 105280.

Ziajahromi S, Drapper D, Hornbuckle A, Rintoul L, Leusch FDL. Microplastic pollution in a stormwater floating treatment wetland: Detection of tyre particles in sediment. Science of The Total Environment 2020; 713: 136356.

Ziajahromi S, Neale PA, Rintoul L, Leusch FDL. Wastewater treatment plants as a pathway for microplastics: Development of a new approach to sample wastewater-based microplastics. Water Research 2017; 112: 93-99.